Soft Matter

Dynamic Article Links

Cite this: *Soft Matter*, 2012, **8**, 8972

www.rsc.org/softmatter

PAPER

Induced dye leakage by PAMAM G6 does not imply dendrimer entry into vesicle lumen†

Anna Åkesson,*[a] Christian Veje Lundgaard,[b] Nicky Ehrlich,[b] Thomas Günther Pomorski,[c] Dimitrios Stamou[b] and Marité Cárdenas*[a]

Received 13th April 2012, Accepted 20th June 2012
DOI: 10.1039/c2sm25864a

Dendrimers are polymers with unique properties that make them promising in a variety of applications such as potential drug and gene delivery systems. Polyamidoamine (PAMAM) dendrimers, in particular, have been widely investigated since they enter rapidly into cells. The entry mechanism, however, is still not yet fully clarified as both passive and active uptake have been proposed. In this work we focus on understanding passive uptake, for which simple cell model systems are used in order to ensure that only dendrimer–lipid interactions are probed. We developed protocols for investigating independently the effect of the dendrimer on lipid bilayer integrity, in terms of permeability of small dyes and effective dendrimer translocation. This was achieved by the use of membrane labeled giant unilamellar vesicles (GUVs) either containing Alexa 488 hydrazide in the vesicle lumen or FITC-labeled PAMAM G6 dendrimers. Vesicle integrity and dendrimer–membrane binding were then assessed by fluorescence microscopy. The importance of membrane fluidity and charge was investigated using GUVs composed of various lipid compositions. A quartz crystal microbalance with dissipation was used to probe the effect of dendrimers on the rigidity of vesicle layers. The results indicate that PAMAM dendrimers can locally alter the membrane properties. An increased bilayer permeability towards soluble small dyes but no effective translocation, where PAMAM dendrimers could dissociate from the lipid membrane into the vesicle lumen, was observed. To our knowledge this is the first time it is shown that PAMAM G6 dendrimer does not effectively translocate the lipid bilayer although it readily interacts with the model membrane, regardless of lipid membrane properties. However, bilayer charge and fluidity modulate the dendrimer interaction in agreement with previous reports. The results clearly highlight the importance of the choice of the model system when investigating nanoparticles interaction with lipid membranes.

Introduction

Polyamidoamine (PAMAM) dendrimers are monodisperse hyperbranched polymers with amido amines as building blocks. The regular branching leads to a globular structure where each new set of branches provides an additional shell on the surface (or generation). Because of this exponential growth, dendrimer molecules can become quite large, with sixth generation structures showing sizes in the same range as medium sized proteins (*ca.* 7 nm diameter). PAMAM dendrimers were synthesized and characterized for the first time in 1985 by Tomalia *et al.*[1] and since then several applications in the medical field have been proposed including drug/gene delivery and MR imaging.[2–8] In the field of drug delivery, dendrimers are mainly used to improve solvability of hydrophobic drugs and increase the activity and bioavailability of the drugs.[7] Dendrimer's ability to penetrate cell membranes is the main factor responsible for increasing activity of the drug complex. Although this subject has been studied extensively *in vitro*, it is still not fully understood how dendrimers interact with, and are transported through, cell membranes. Some studies suggest that PAMAM dendrimers are internalized in cells through the caveloae or clathrin pathway although they may also be able to passively translocate across the cell membrane without the aid of protein pathways.[9–12] PAMAM dendrimers show increased reactivity with increasing generation both in model membranes and *in vitro* studies.[12–14] Earlier studies

[a]*Institute of Chemistry and Nano-Science Center, University of Copenhagen, Universitetsparken 5, DK 2100 Copenhagen, Denmark. E-mail: cardenas@nano.ku.dk; aakesson@nano.ku.dk*
[b]*Bionanotechnology and Nanomedicine Laboratory, Department of Chemistry, Nano-Science Center and Lundbeck Foundation Center for Biomembranes in Nanomedicine, University of Copenhagen, Denmark*
[c]*Center for Membrane Pumps in Cells and Disease – PUMPKIN, Department of Plant Biology and Biotechnology, University of Copenhagen, Thorvaldsensvej 40, DK-1871 Frederiksberg C, Denmark*
† Electronic supplementary information (ESI) available: Additional fluorescent microscopy images, spectrofluorescence measurements on FITC-labeled dendrimers and additional QCM-D experiments. See DOI: 10.1039/c2sm25864a

on supported lipid bilayers (SLBs) and small unilamellar vesicles (SUVs) found that bilayer fluidity is crucial for hole formation[15–17] but currently there is no clear consensus on the dendrimer generation required for this hole formation. For SLB,[18,19] for instance, PAMAM G3 only accumulated on membrane defects while larger generations expanded pre-existing defects or induced new defects. These discrepancies may arise from the wide variety of ionic conditions used in previous reports that ranged from pure water[19] to buffer enriched with salt.[13,15,17,20]

Here we present an alternative approach to study nanoparticle interaction with model cell membranes. In this approach, we make use of giant unilamellar vesicles (GUVs) tethered to a solid support *via* biotin–avidin linkages.[21] In this way, the vesicles have sizes in the range of typical cells (5–15 μm) and should not be subject to major mechanical strains since the contact with the surface is restricted to a low number of linkers per surface area (~800 linkers per μm^2). Fluorescence microscopy is used to probe whether dendrimers are able to alter the lipid membrane structure by monitoring the release of a water soluble dye (Alexa 488 hydrazide) encapsulated in the lumen of the vesicles and membrane interaction of FITC-labeled dendrimers. Additionally, SUVs were used to probe the effect of dendrimers on the rigidity/elasticity of vesicles by means of a quartz crystal microbalance with dissipation (QCM-D). Our studies indicate that PAMAM dendrimers of generation six can efficiently change the membrane permeability of zwitterionic fluid phase bilayers while no increase in permeability is seen for neutral bilayers in the gel phase. Furthermore, addition of a negative charge to the membrane enhances the interaction with the highly cationic PAMAM dendrimers. QCM-D experiments prove that PAMAM dendrimers change the viscoelastic properties of the vesicles, which may be an explanation for the enhanced permeability observed in the fluorescence microscopy studies.

Experimental

Materials

1-Palmitoyl-2-oleoyl-*sn-glycero*-3-phosphocholine (POPC), 1,2-dipalmitoyl-*sn-glycero*-3-phosphocholine (DPPC), 1-palmitoyl-2-oleoyl-*sn-glycero*-3-phospho-(1′-*rac*-glycerol) (POPG) and 1,2-dioleoyl-*sn-glycero*-3-phosphoethanolamine-*N*-cap biotinyl (DOPE-Biot) were used as received from Avanti Polar Lipids Inc. (Birmingham, AL, USA). 1,2-Dipalmitoyl-*sn-glycero*-3-phospho-(1′-*rac*-glycerol) (DPPG) purchased from Larodan Fine Chemicals (Malmö, Sweden) was also used as received. All lipids stored in chloroform and kept at −20 °C. 1,1′-didodecyl-3,3,3′,3′-tetramethylindocarbocyanineperchlorate (DiIC12), 1,1′-dioctadecyl-3,3,3′,3′-tetramethylindodicarbocyanineperchlorate (DiDC18) and Alexa Fluor® 488 hydrazide (Alexa) from Invitrogen (Paisley, UK) were likewise used without further purification. Unless indicated otherwise, all other chemicals and reagents were obtained from Sigma-Aldrich A/S (Copenhagen, Denmark). The PAMAM dendrimer, ethylenediamine core, generation 6.0 was purchased in methanol. Before use, methanol was evaporated under reduced pressure and the dendrimer was resolubilized in phosphate salt buffer (PBS) containing 100 mM NaCl, 8.1 mM Na_2HPO_4, and 1.9 mM NaH_2PO_4, pH 7.4. Milli-Q purified water was used in all experiments. Physical properties of the main components are shortly described in Table 1.

Table 1 Physical properties of the main components under the experimental conditions used in this work[a]

Molecule	Surface charge	T_m (°C)	Reference
POPC	Zwitterionic	−2.0	22
DPPC	Zwitterionic	41.6	23
POPG	Anionic	−5.3	24
DPPG	Anionic	40.0	23
PAMAM G6	Cationic	—	

[a] T_m, phase transition temperature.

Fluorescein isothiocyanate-labeling of dendrimers

Fluorescein isothiocyanate (FITC) was covalently conjugated to the amine groups of the dendrimers through the formation of thiourea bonds. Briefly, FITC dissolved in methanol was slowly added to the dendrimer solution in a molar ratio of 1 : 1.2 dendrimer : FITC. Unreacted FITC was removed by dialysis against PBS buffer for 2 d or until no free dye was observed in the dialysis buffer. Attachment of FITC to dendrimers was verified by spectrofluorimetry (excitation at 475 nm; emission at 583 nm) using a Fluoromax-4 (Horiba, Edison New Jersey, USA), see Fig. SI2.† An average molar ratio of 1 : 0.7 dendrimer : FITC was obtained.

GUV preparation

GUVs were prepared by gentle hydration of lipid films according to previous protocols.[25,26] Briefly, lipids were mixed in small glass vials with DiD-C18 and DOPE-biotin in chloroform to give 1 and 0.5 mol%, respectively. A thin lipid film was prepared by drop-by-drop addition of the mixture to small Teflon cups. The remaining chloroform was removed by storing the Teflon cups in a vacuum-chamber for 30 min. Lipids were rehydrated in D-sorbitol solution (46.1 g l^{-1} in PBS) to a lipid concentration of 0.5 mg ml^{-1}. Lipid mixtures containing DPPC were then incubated overnight at 52 °C while all other lipid solutions were kept at 37 °C. After one night of incubation all vesicles were stored at 4 °C for a maximum of one week before use.

SUV preparation

Small unilamellar vesicles (SUVs) were prepared by pressurized extrusion. Briefly, lipids were mixed in small glass-vials to achieve the desired molar ratio 75 : 25 : 0.5 POPC : POPG : DPPE-biotin. A thin lipid film was created by evaporation of chloroform under a stream of N_2 followed by incubation in a vacuum chamber for 30 min. The lipid film was hydrated with PBS buffer, filtered through 0.2 μm filters (Sartorius, Goettingen, Germany), for 1 h at ambient temperature prior to five freeze–thaw cycles using liquid nitrogen and a water bath at 30 °C. The lipid vesicle solution was then extruded 10 times through 0.05 μm filters (Merck Millipore, Billerica, USA) using a Lipex™ pressurized extruder (Northern Lipids Inc., Vancouver, Canada).

Fluorescence microscopy imaging

Microscopy imaging was performed on an inverted confocal microscope TCS SP5 (Leica, Wetzlar, Germany) and a wide field

microscope AF6000LX (Leica). For confocal microscopy a 100× (numerical aperture 1.34) oil-immersion objective HCX PL APO was used. In fluorescence microscopy Alexa and FITC labeled dendrimers were excited with a 488 nm argon laser and emission was captured between 491 and 563 nm. Lipid dyes DiDC18 and DiIC12 were excited with 633 nm and 543 nm lasers and recorded between 640–700 and 550–582 nm, respectively. For wide field microscopy a 63× (numerical aperture 1.0) water immersion objective was used. A mercury lamp with filter cubes EGF cube 49002 ET, EC3 cube 49004 ET, and EC5 cube 49006 ET (Chroma Technology Corp, Bellows Falls, USA) was used to excite Alexa/FITC, DiI-C12 and DiD-C18, respectively. Glass coverslips were cleaned by copious sonication cycles in 2% (v/v) Hellmanex (Hellma Analytics, Germany) and water, plasma-etched and mounted in microscopy chambers prior to biotin–BSA–streptavidin functionalization. For surface functionalization, 1.0 g l^{-1} BSA–biotin : BSA (1 : 10) was added to the surface and incubated at ambient temperature for 10 min. After five times gentle washing with PBS, streptavidin (0.025 g l^{-1} in PBS) was added and likewise incubated for 10 min followed by five times washing with PBS. Prior to imaging GUVs were added to the microscopy chamber to a final lipid concentration of 0.01 g l^{-1} and allowed to stabilize for at least 30 min before the measurement. Several GUVs were imaged in each experiment and all experiments were reproduced at least three times. Note that the total concentration is just an estimate since it is hard to control the exact volume and the mass transfer conditions of the surface in this open cell setup. The illumination intensity and exposure time were changed between the experimental setups to maximize the signal.

Quartz crystal microbalance with dissipation (QCM-D)

QCM-D measurements were performed with a Q-SENSE E4 system (Q-Sense, Västra Frölunda, Sweden). The sensor crystals used were silicon oxide, 50 nm (Q-Sense). For cleaning, the sensor surfaces were placed in 2% Hellmanex for 10 min followed by thorough rinsing in absolute ethanol and ultrapure water. The surfaces were dried in a stream of nitrogen and oxidized in a UV-ozone chamber (BioForce Nanosciences, Inc., Ames, IA) for 10 min in order to remove molecular levels of contamination. O-rings were placed in 2% Hellmanex for 10 min followed by careful rinsing in ultrapure water and drying in a stream of nitrogen. The sample cells were quickly assembled to avoid contamination. Before measurements the instrument temperature was set at 25 °C and allowed to equilibrate. The fundamental frequency and six overtone frequencies (3^{rd}, 5^{th}, 7^{th}, 9^{th}, 11^{th}, 13^{th}) were found in air and a stable baseline was recorded. PBS buffer was introduced into the flow cells using a peristaltic pump (Ismatec IPC-N 4) at a flow rate of 100 μl min^{-1}. Surfaces were then functionalized similar to the microscopy chambers, using neutravidin instead of streptavidin. Briefly, 1.0 g l^{-1} BSA–biotin : BSA (1 : 10) was flowed through the cells and allowed to incubate for 10 min. After extensive rinsing with PBS, neutravidin solution (0.025 g l^{-1} in PBS) was added and likewise incubated for 10 min. This was followed by washing with PBS (10 min) before extruded vesicles were flowed through the cell at a lipid concentration of 0.2 mg ml^{-1}. Before addition of PAMAM G6 dendrimers excess vesicles were rinsed off using PBS buffer.

Results

Effect of membrane fluidity

First, we studied the interaction of PAMAM dendrimers with Alexa-loaded GUVs composed of either pure 1-palmitoyl-2-oleoyl-*sn-glycero*-3-phosphocholine (POPC) or 1,2-dipalmitoyl-*sn-glycero*-3-phosphocholine (DPPC), which at room temperature are in the fluid or gel phase, respectively. The results are displayed in Fig. 1. For gel phase GUVs, vesicle integrity was not affected by dendrimer addition; no leaking of the soluble dye was observed even up to 1 h after addition of 10 μM dendrimer solution (Fig. 1A and B). For fluid phase GUVs, on the other hand, leakage was observed within 15 min after addition of 10 μM dendrimer solution (Fig. 1C and D). Thus, PAMAM dendrimers are more prone to cause leakage with lipid membranes in the fluid phase than in the gel phase in agreement with previous results based on SLB[15,16] and Langmuir films.[17] Lipid molecules in fluid phase bilayers are more tilted, resulting in a larger head group area compared to lipids in gel phase bilayers. Moreover, the lipids are highly mobile in a fluid phase bilayer and can thus respond to match the dendrimer surface charges. This could to some extent explain why dendrimers preferably interact with fluid phase bilayers. Control experiments, where only the buffer was added to the vesicles (Fig. SI1†), showed no change in vesicle permeability.

In order to test whether PAMAM dendrimers accumulate on and cross GUV membranes to be released into the vesicle's lumen, FITC-labeled dendrimers were used instead. To ensure a minimal modification of the FITC functionalization on the activity of the PAMAM G6 dendrimers, a very low FITC/dendrimer ratio was used in such a way that only 3 out of 4 dendrimers carried 1 FITC molecule on their surface (see discussion regarding Fig. SI2†). Moreover, the signals for FITC labeled and unlabeled dendrimers gave comparable responses in QCM-D experiments (see Fig. SI9† and discussion therein). Upon addition of FITC-labeled dendrimers to GUVs, no significant increase in the FITC signal was detected at the vesicle membrane or inside the vesicle lumen (Fig. 1E and F). Taken together, these experiments show that PAMAM G6 dendrimers are able to alter the structure of the lipid membrane allowing rapid passage of small molecules without dendrimer translocation into the vesicle lumen, given that the lipids in the membrane are mobile enough.

Effect of phase coexistence

Next, we tested whether steep edges between coexisting phase domains could promote dendrimer interaction since dendrimers were shown to interact with SLB mainly by expanding already existing defects in the bilayer.[16,18,20,27] GUVs were prepared from DPPC–POPC (80 : 20, molar ratio), a lipid mixture that results in coexisting fluid and gel phase domains at room temperature (Fig. SI3,† ref. 22 and 28). Similar to fluid POPC vesicles, dendrimers were able to promote leakage of the small dye (Fig. 1G and H) but no significant difference in the number of leaked vesicles or the rate of leaking could be detected between GUVs composed of DPPC–POPC and pure POPC (Fig. SI4†). These results suggest that the dendrimer does not seem to display a preference towards irregularities on the lipid bilayer (the edge of the coexisting domains). Similar to pure POPC vesicles no signal

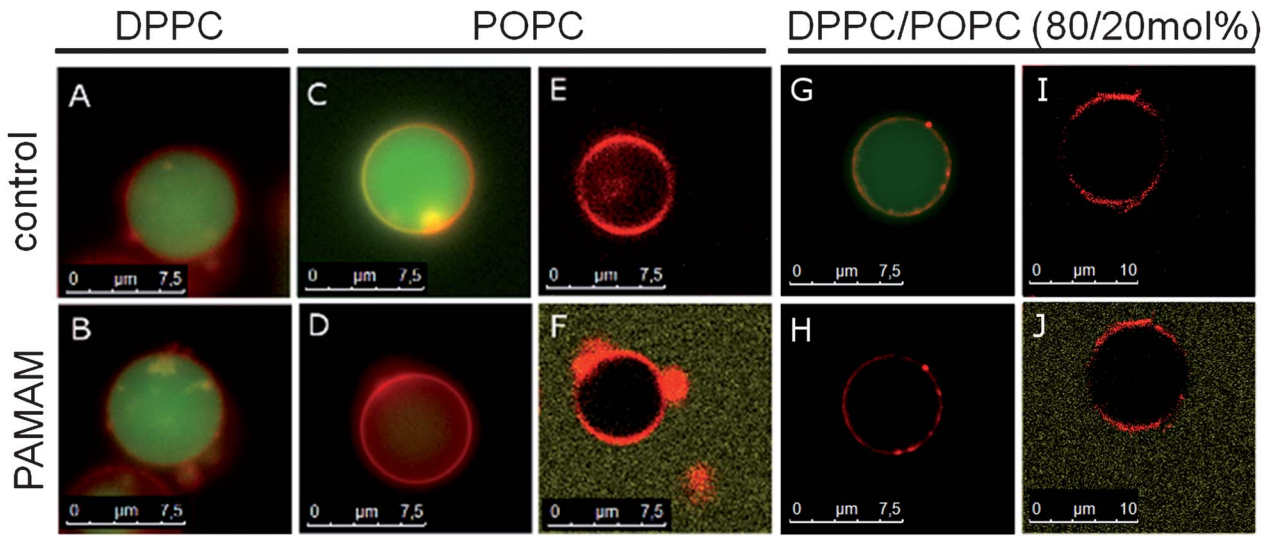

Fig. 1 PAMAM G6 interaction with DPPC (gel phase) and POPC (fluid phase) membranes. GUVs were prepared from the indicated lipids. DiD-C18 (red) was used to visualize the membranes. In (A–D) and (G and H), Alexa 488 (green) was used to visualize the vesicle aqueous lumen. Vesicles were analyzed by fluorescence microscopy before (control) and after addition of 10 µM PAMAM G6. In (F) and (J), FITC-labeled PAMAM G6 was added. For clarity, only one vesicle representing the overall result is shown in each image.

from FITC-labeled dendrimers could be observed inside the vesicle lumen (Fig. 1I and J).

Effect of membrane charge

Most biological membranes carry a net negative charge[29] and are, due to attractive electrostatic forces, expected to interact more strongly with the highly cationic PAMAM dendrimers than the neutral PC bilayer. In Fig. 2, we study the effect of PAMAM dendrimers in addition to GUVs composed of a binary mixture of POPC and phosphatidyl glycerol (POPG) at a molar ratio of 3 : 1, matching the charge of the cell membrane of typical Gram positive bacteria.[30] POPG only differs from POPC in its head group structure, thus any change in the mechanism of interaction can be directly correlated with an increased surface charge density of the vesicles. As expected, the dendrimers showed a higher affinity towards negatively charged POPG-containing GUVs as compared to GUVs composed of pure POPC since they not only induced content leakage (Fig. 2A and B) but also substantially accumulated at the vesicle surface (Fig. 2C and D).

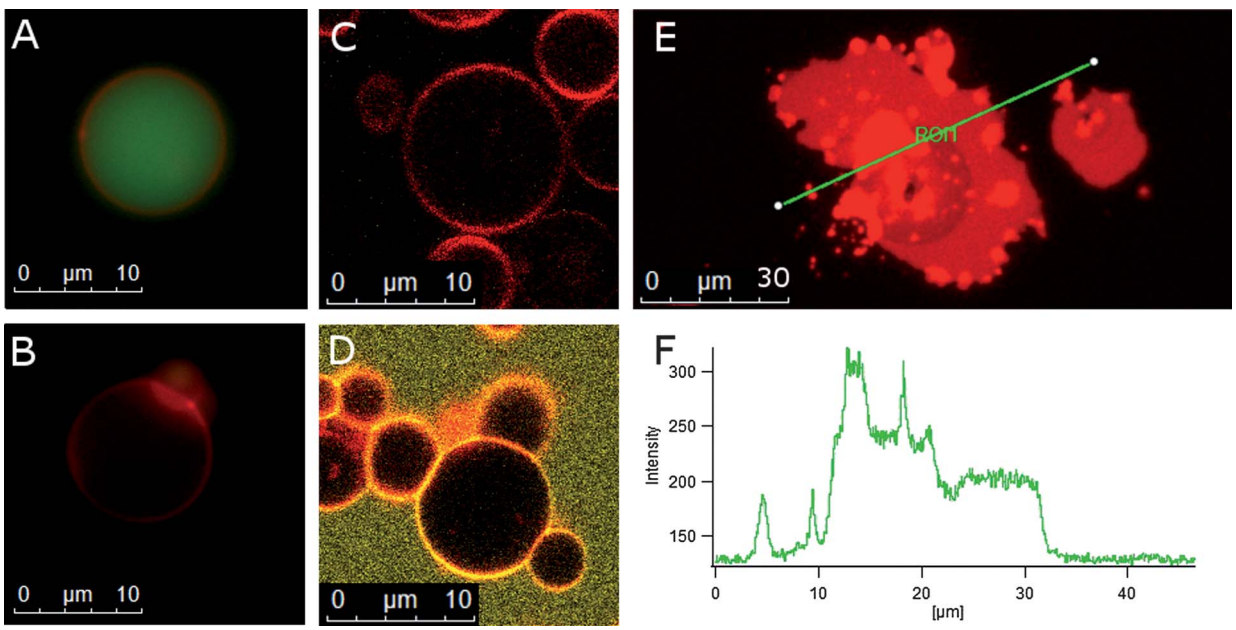

Fig. 2 PAMAM G6 interaction with negatively charged POPC/POPG membranes. GUVs were prepared from the POPC/POPG mixture (75 : 25, molar ratio). DiD-C18 (red) was used to visualize the membranes. In (A) and (B), Alexa 488 (green) was used to visualize the vesicle aqueous lumen. Vesicles were analyzed by fluorescence microscopy before (A and C) and after addition of 10 µM unlabeled PAMAM G6 (B) or 10 µM FITC-labeled PAMAM G6 (yellow, D). During incubation with 10 µM PAMAM G6 dendrimers some vesicles collapsed on the glass surfaces (E). An intensity line profile obtained from the marked line is shown in (F).

Similar to POPC vesicles, no significant translocation of the fluorescently labeled dendrimer inside the vesicle lumen was detected upon incubation with 10 μM PAMAM G6 (Fig. 2D). In the latter case, an increase of vesicle aggregation over time was observed (Fig. 2C and D) followed by collapse of several vesicles onto the glass surface (Fig. 2E). Fig. 2F gives a line profile over the collapsed vesicles shown in Fig. 2E; discrete intensity increments are observed suggesting that stacks of lipid bilayers are formed. Co-localization of dendrimer and lipid signals (Fig. SI5†) suggests that dendrimers are situated in close contact with the lipid membranes in line with results from SAXS studies of the condensed lamellar gel phase.[31]

Interestingly, a significant increase in FITC-labeled dendrimers was observed around the POPG containing membrane but not around the pure POPC vesicle (Fig. 3 and SI7†). Regardless of the lipid composition, no significant signal from FITC labeled dendrimers could be detected inside the vesicle lumen. Thus, even though dendrimers are able to interact with the lipid bilayer, they are not able to dissociate from the membrane and enter into the vesicle lumen.

Dendrimer accumulation on the negatively charged membrane agrees with stronger attractive electrostatic forces between the cationic dendrimers and the anionic membrane. Although no increased dendrimer concentration was found around pure POPC membranes, our leakage studies prove dendrimer interaction with these membranes. Thus, even though dendrimers also associate with the POPC bilayer the attraction is not strong enough to create significant dendrimer accumulation on the bilayer surface within the experimental time (1 h). In line with our results Tiriveedhi *et al.*[17] reported a decrease in dissociation constant between the PAMAM dendrimer and bilayer for negative bilayers compared to the neutral ones, leading to accumulation of dendrimers on the negatively charged bilayer surface. Dendrimer adsorption and accumulation on the lipid bilayer may locally change the curvature of the lipid bilayer, thereby altering the membrane density. This would explain an increased permeability towards smaller dyes while no translocation of the dendrimer occurred. Molecular dynamics simulations and Raman spectroscopy studies have shown that dendrimers can be fully or partly incorporated into the lipid bilayer thus altering the bilayer structure and fluidity.[15,27,32]

Interestingly, dendrimer exposure to GUVs composed of DPPC–DPPG (75 : 25 molar ratio) leads to both release of lumen dye and dendrimers accumulation at the GUVs surface (Fig. SI6†). No significant dendrimer translocation into the vesicle lumen was detected for this composition either. The fact that dendrimer accumulation leads to induced leakage in gel phase vesicles containing 25 mol% DPPG indicates that the negative surface charge density in these vesicles is high enough not to require local charge rearrangements and thus lipid mobility. Moreover, the uneven fluorescence signal from both lipids and dendrimers on the vesicle surface (Fig. SI6†) seems to suggest that DPPC–DPPG form domains and thus the local DPPG concentration in close vicinity to the dendrimers might be higher than 25%. These results are in agreement with Langmuir film balance studies where non-ideal mixing has been reported for these lipids.[33,34]

Effect on membrane elasticity

Dendrimer adsorption to the lipid bilayer induces local changes in the bilayer curvature[35] and flattening of the lipid membrane in SUVs,[31] which improves the contact between neighboring vesicles upon dendrimer bridging. These changes in the lipid membrane structure may induce a change in the mechanical properties of the lipid membrane, resulting in changed permeability. The change in membrane elasticity upon dendrimer binding could for instance be measured by following the contact angle or line tension between vesicles and the surface using reflection interference contrast microscopy, RICM (for a review see Limozin and Sengupta[36]). In this study we have instead chosen to use a QCM-D since this is an excellent technique to probe viscoelastic properties of adsorbed films.[37,38] The QCM-D signal is characterized by a change in frequency and dissipation,

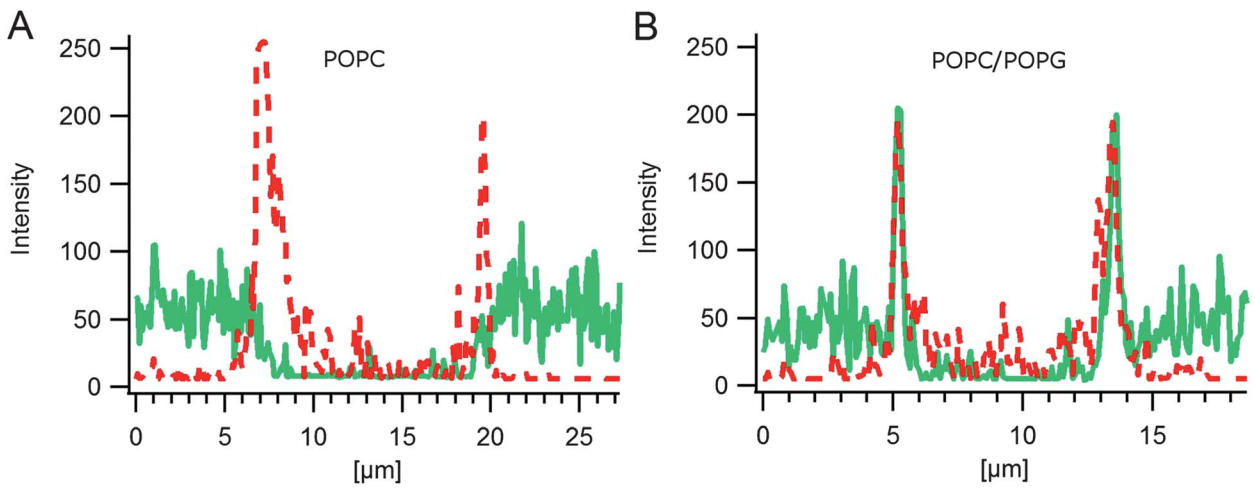

Fig. 3 Analysis of PAMAM dendrimer interaction with charged and uncharged GUVs. Fluorescence intensities of DiD-C18-labeled GUVs composed of either POPC alone (A) or POPC–POPG, 75 : 25 molar ratio (B) after addition of 10 μM FITC-labeled PAMAM G6 dendrimers were taken from averaged confocal images through the equatorial plane. The signal from membrane dye DiD-C18 is shown as a dashed red line and that from FITC-labeled dendrimers is shown as a solid green line. The original microscopy images are given in Fig. SI7.†

which are related to the properties of the adsorbed film. When a film adsorbs to the crystal surface, the total mass of the crystal will increase with a consequent decrease in resonance frequency. If the adsorbed layer is soft/viscous (as for SUVs), the film will not follow the crystal oscillations perfectly giving rise to internal friction due to deformation and therefore an increase in dissipation.

Given that more dramatic effects on the structure of vesicles occur for POPG containing vesicles as compared to pure POPC GUVs, we decided to investigate the effect of dendrimer addition to SUVs composed of 75 : 25 mol% POPC–POPG using a QCM-D (Fig. 4). Vesicles containing a biotin labeled lipid were exposed to a pre-coated neutravidin surface (at time −8000 s), where vesicle tethering leads to a large change in frequency and dissipation in agreement with the formation of viscous layers.[39–42] PAMAM dendrimers were then added to the vesicles at time 0 s and the change in frequency and dissipation was recorded over time. Interaction of PAMAM G6 dendrimers with SUVs showed a complex dendrimer concentration-dependent mechanism. The different steps in the mechanism are most easily identified by plotting dissipation *versus* frequency as shown in Fig. 4C. The interaction mechanism can be divided into 3 distinct processes:

(1) Initially there was a dendrimer concentration independent regime that induces a large decrease in dissipation without significant changes in frequency. This corresponds to stiffening of the adsorbed layer (or lipid membranes) upon dendrimer binding. Since the change in frequency is almost insignificant, stiffening occurs at quite low dendrimer concentrations on the vesicle surface.

(2) Secondly, there was a significant change in both frequency (increase) and dissipation (decrease). This behavior is typically attributed to layer desorption. Desorption could be a result of either vesicle collapse where a large amount of entrapped water is released,[43,44] similar to vesicle fusion during formation of SLB, or it could also be due to partial detachment of vesicles from the surface.

(3) Finally, a large increase in dissipation and decrease in frequency were observed. The onset of this stage is dendrimer concentration dependent. This is typically correlated with the formation of an adsorbed film of viscous structures.[39–42] This final step is in agreement with the formation of large multilamellar structures as those observed in Fig. 2E, F and SI4.†

Control experiments were run by adding PAMAM G6 dendrimers to a precoated neutravidin layer in the absence of SUVs and gave a very small decrease in dissipation and increase in frequency (−0.5 and +3 Hz, respectively). Thus, the observed change in frequency and dissipation in the presence of SUVs cannot be attributed to dendrimer binding to the protein-coated surface.

Discussion

We have found that both membrane charge and membrane fluidity are important for the interaction of generation six PAMAM dendrimers with lipid membranes. Dendrimers caused vesicle leakage and accumulated strongly on negatively charged membranes containing 25 mol% PG lipids in agreement with previous studies, where a decrease in dissociation constant between the PAMAM dendrimer and bilayer was found for negative bilayers compared to the neutral ones.[17] Although the electrostatic interaction between negatively charged lipids and the PAMAM dendrimer might be the main driving force, also other factors seem to promote dendrimer interaction with lipid membranes since leakage was observed also for zwitterionic POPC vesicles. Indeed, Kelly *et al.*[35] measured the enthalpy of interaction between PAMAM dendrimers and SUVs of different

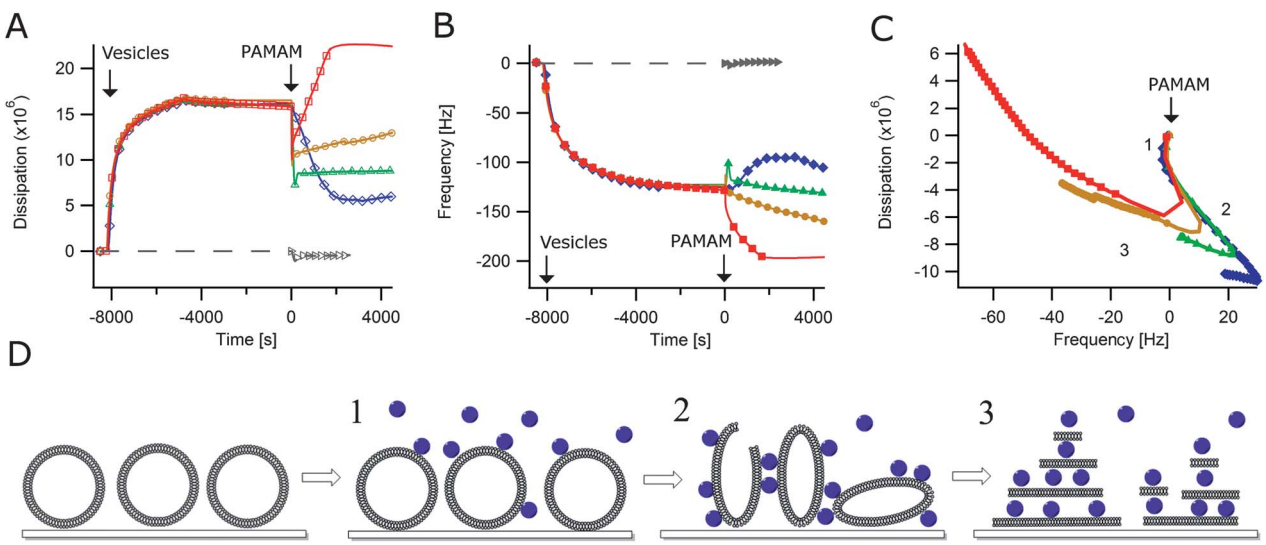

Fig. 4 Analysis of PAMAM dendrimer interaction with charged SUVs by a QCM-D. Changes in dissipation (A) and frequency (B) are given as a function of time for the 7th overtone. Vesicle binding to the surface *via* biotin–neutravidin linkage ($t = -8000$ s) results in a large increase in dissipation and decrease in frequency. At time $t = 0$ s, the tethered vesicles are exposed to 0.01 μM (◇, blue), 0.1 μM (△, green), 1 μM (○, yellow) or 10 μM (□, red) PAMAM G6 dendrimer. Exposure of the linkage functionalized surface without tethered vesicles to 1 μM PAMAM G6 is shown in grey. The effect of dendrimer addition on frequency (ΔF) and dissipation (ΔD) is complex and concentration dependent, and can be most easily understood by plotting $\Delta D/\Delta F$ as given in (C). For simplicity, in the latter case ΔD and ΔF are calculated with respect to time $t = 0$, and no data prior to dendrimer addition are shown. Schematics drawn to scale for the different mechanism steps are given in (D). Data for a complete experiment are shown in Fig. SI8.†

charges, and found that there was an exothermic reaction for negatively charged lipids while the reaction was endothermic for neutral and positively charged bilayers at low dendrimer/lipid molar ratios. Polyelectrolytes in the presence of oppositely charged molecules and surfaces are known to interact *via* entropically driven forces, given the release of a large amount of bound counterions and the consequent increase in the translational entropy of the system.[45] The dipolar moment of PC lipid membranes might be enough to partially neutralize some of the dendrimer charges and thus the counterion release might be the driving force for dendrimer–zwitterionic membrane interaction.

In order to minimize the free energy of the system, both the dendrimers and the bilayers are likely to deform to maximize the contact between the charged terminal groups of the PAMAM molecule and the lipid head groups. Several interaction mechanisms have previous been proposed. Among those dendrisome formation was proposed for high generation dendrimers,[19,20,46] in which the dendrimers are encapsulated by the lipid membrane. This structure should not be energetically favored for the PAMAM G6 molecule due to the high curvature needed for the bilayer to encapsulate the dendrimers.[19] Furthermore, the formation of a dendrisome should produce a high degree of dendrimer translocation in our experiments, similar to the invagination of vesicles upon endocytosis. Another possible scenario for increased lipid–dendrimer interaction would be dendrimer deformation at the membrane surface as observed for small generation (<G6) dendrimers.[35,46,47] Due to steric hindrance of dendrimer branches with increasing dendritic generation,[48,49] large dendrimer deformation is not likely to occur for PAMAM G6 molecules. A third proposed mechanism involves dendrimer aggregation on the membrane surface without significantly altering the shape of the dendrimers.[19,35] For instance, several smaller dendrimers could aggregate to have the same size and charge as larger generations and lead to a change in membrane curvature. The electrostatic repulsion between the dendrimers would have to be compensated if such aggregates do exist, and thus this structure is less energetically favorable.

We propose an alternative mechanism of interaction for dendrimers binding to the lipid vesicle. The matching of the charges between the lipid bilayer and the PAMAM dendrimers for partial neutralization of the dendrimer charges and the consequent counterion release require a fluid membrane for lipids to diffuse and rearrange, hence locally reducing the bilayer density and inducing local defects. This leads to an increased permeability towards small dye molecules and leakage from the vesicle lumen (Fig. 1 and 2). A similar leakage of soluble dyes has been observed upon vesicle fusion due to mechanical bridging between two complementary DNA strands between vesicles.[50] However, fluidity of the membrane is not a determining factor when the membrane charge density is high enough to match the surface charge of the dendrimers in the contact region (Fig. SI6†). Since half of the dendrimer charges are free to interact with more lipids and due to the inability of the lipid bilayer to follow the dendrimer curvature, bridging between vesicles is favored in particular for the POPG containing membranes where large range electrostatic forces are important (Fig. 2D). Cryo-TEM performed in our group on SUVs of similar composition shows that linkage of the vesicles alters the membrane curvature.[31] Dendrimer binding produces increased vesicle stiffness as assessed *via* a QCM-D (Fig. 4 and SI8†) even at very dilute dendrimer concentrations as compared to the conditions used in fluorescence microscopy experiments (Fig. 2). Stiffening of the vesicles makes them unstable and induces their collapse on the surface. Indeed, stacking of lipid bilayers observed in Fig. 2E, F and SI5† resembles the lamellar gel phase obtained upon phase separation in the bulk.[31] Although, high line tension between the membrane and the surface could facilitate vesicle collapse upon dendrimer adsorption, due to the low percentage of biotin linkers we believe that the line tension should only have a minor effect as reported by Bendix *et al.*[51]

Bridging of negatively charged vesicles with PAMAM dendrimers was also proposed by Zhang and Smith[52] who observed enhanced lipid mixing upon dendrimer addition. For supported lipid bilayers local changes in membrane curvature and stiffness may lead to some lipids being dragged out of the bilayers, consistent with hole formation observed using AFM.[16,18,20]

Our results indicate that PAMAM G6 dendrimers are unlikely to translocate across the membrane and be released into the vesicle lumen as a result of nonspecific interactions. However, due to the resolution of the microscope we were unable to determine whether the dendrimers translocate but stay attached to the membrane. In order to verify this very important issue, other high resolution techniques must be used. We are currently performing neutron reflectivity studies on SLB under similar experimental conditions as the ones used in this work. Neutron reflectivity is a surface sensitive label free technique with a resolution down to 5 Å when using the contrast matching method. This technique should finally allow us to tell whether the dendrimers translocate or get intercalated across the membrane.

Since the molar ratios at which vesicle collapse is observed are far above those used in cell studies,[10,12,53] the observed translocation in living cells must be due to biologically active processes or other unknown interactions as for instance the formation of complexes with soluble proteins present in the cell medium as observed for several other nanoparticles.[54–56]

Notably, exposure of low to moderate PAMAM dendrimer concentrations[57] to red blood cells leads to aggregation and cellular morphology changes. Indeed, incubation with 156 μM PAMAM G5 caused lysis of red blood cells.[58] From our studies it is clear that the observed changes in the shape of red blood cells and their eventual collapse at high dendrimer concentrations might be related to dendrimer induced changes in the mechanical properties of the membrane, where the cell membrane reflects the properties of dendrimer layers rather than those of the lipid bilayer.

Finally, this study demonstrates the importance of choosing a model system correctly: although leakages from lipid vesicles and cells are often used to assess dendrimer translocation,[13,17] this seems to be a poor indicator of actual dendrimer translocation. Studies on SLB in which large holes were induced by exposure to dendrimers[13,59,60] are misleading since formation of static holes as an effect of lipid removal is more likely to occur on SLB than real cells and vesicles where the membrane can close eventual holes. Moreover, our study clearly demonstrates that leakage of small soluble dye inside the lumen of SUV does not necessarily correlate with dendrimer translocation into the vesicle lumen. The appropriate choice of the model system is of importance

when studying possible interaction mechanisms with the aim of creating and improving drug and gene delivery vehicles. Our study also shows that membrane fluidity is of great importance for membrane rearrangement caused by PAMAM dendrimers. This would be of great importance in cell studies where active *versus* passive translocation of PAMAM dendrimers and cell leakage is investigated at 37 °C and 4 °C, respectively.[53,60] Such drastic changes in temperature would also affect the membrane fluidity,[61,62] shown here to have a great impact on dendrimer interaction and thus should be carefully considered when studying nanoparticle interaction with membranes.

Conclusions

Using GUVs we have shown that both membrane fluidity and charge density are of great importance for PAMAM G6 dendrimer interaction. Only when the neutral bilayer contains lipids in the fluid phase does the permeability change sufficiently for small molecules to be able to translocate across the membrane. Using fluorescently labeled dendrimers we have shown that dendrimers bind and accumulate on the surface of PG-containing vesicles while no such accumulation occurs for PC lipids. It is shown here for the first time to the authors' knowledge that no significant translocation and release of PAMAM G6 into the vesicle lumen occur, under the same conditions where dendrimers are able to increase bilayer permeability towards small molecules. Thus, any transient hole in the membrane is by no means larger than the diameter of G6 PAMAM dendrimers (7 nm). Increasing the negative charge density in the bilayer favors dendrimer interaction since dendrimers more readily accumulate at the vesicle surface. Analysis by a QCM-D revealed that dendrimer binding causes stiffening of the vesicles leading to vesicle destabilization and vesicle collapse in agreement with fluorescence microscopy results. In agreement with previous studies,[17,35] our results indicate that the main driving force for dendrimer interaction with the lipid bilayer is the electrostatic force, although other forces may be involved in the interaction as for instance the entropic contribution from multi-ion counter ion release. Our study provides evidence of the importance of the choice of a model system when studying possible interaction mechanisms with the aim of creating and improving drug and gene delivery vehicles.

Acknowledgements

The authors gratefully acknowledge the financial support from "Center for Synthetic Biology" at Copenhagen University funded by the UNIK research initiative of the Danish Ministry of Science, Technology and Innovation.

Notes and references

1 D. A. Tomalia, H. Baker, J. Dewald, M. Hall, G. Kallos, S. Martin, J. Roeck, J. Ryder and P. Smith, *Polym. J.*, 1985, **17**, 117–132.
2 A. Asthana, A. S. Chauhan, P. V. Diwan and N. K. Jain, *AAPS PharmSciTech*, 2005, **6**, E536–42.
3 S. K. Choi, T. Thomas, M. H. Li, A. Kotlyar, A. Desai and J. R. Baker, *Chem. Commun.*, 2010, **46**, 2632–2634.
4 Z. Q. Dong, H. Katsumi, T. Sakane and A. Yamamoto, *Int. J. Pharm.*, 2010, **393**, 244–252.
5 J. Huang, F. Gao, X. X. Tang, J. H. Yu, D. X. Wang, S. Y. Liu and Y. P. Li, *Polym. Int.*, 2010, **59**, 1390–1396.
6 K. Winnicka, K. Sosnowska, P. Wieczorek, P. T. Sacha and E. Tryniszewska, *Biol. Pharm. Bull.*, 2011, **34**, 1129–1133.
7 N. K. Jain and U. Gupta, *Expert Opin. Drug Metab. Toxicol.*, 2008, **4**, 1035–1052.
8 H. Kobayashi, N. Sato, S. Kawamoto, T. Saga, A. Hiraga, T. L. Haque, T. Ishimori, J. Konishi, K. Togashi and M. W. Brechbiel, *Bioconjugate Chem.*, 2001, **12**, 100–107.
9 A. Saovapakhiran, A. D'Emanuele, D. Attwood and J. Penny, *Bioconjugate Chem.*, 2009, **20**, 693–701.
10 O. P. Perumal, R. Inapagolla, S. Kannan and R. M. Kannan, *Biomaterials*, 2008, **29**, 3469–3476.
11 M. Manunta, B. J. Nichols, P. H. Tan, P. Sagoo, J. Harper and A. J. T. George, *J. Immunol. Methods*, 2006, **314**, 134–146.
12 K. M. Kitchens, A. B. Foraker, R. B. Kolhatkar, P. W. Swaan and H. Ghandehari, *Pharm. Res.*, 2007, **24**, 2138–2145.
13 S. Parimi, T. J. Barnes, D. F. Callen and C. A. Prestidge, *Biomacromolecules*, 2010, **11**, 382–389.
14 R. Jevprasesphant, J. Penny, R. Jalal, D. Attwood, N. B. McKeown and A. D'Emanuele, *Int. J. Pharm.*, 2003, **252**, 263–266.
15 B. Erickson, S. C. DiMaggio, D. G. Mullen, C. V. Kelly, P. R. Leroueil, S. A. Berry, J. R. Baker, B. G. Orr and M. M. B. Holl, *Langmuir*, 2008, **24**, 11003–11008.
16 A. Mecke, D. K. Lee, A. Ramamoorthy, B. G. Orr and M. M. B. Holl, *Langmuir*, 2005, **21**, 8588–8590.
17 V. Tiriveedhi, K. M. Kitchens, K. J. Nevels, H. Ghandehari and P. Butko, *Biochim. Biophys. Acta, Biomembr.*, 2011, **1808**, 209–218.
18 P. R. Leroueil, S. A. Berry, K. Duthie, G. Han, V. M. Rotello, D. Q. McNerny, J. R. Baker, B. G. Orr and M. M. B. Holl, *Nano Lett.*, 2008, **8**, 420–424.
19 A. Mecke, I. J. Majoros, A. K. Patri, J. R. Baker, M. M. B. Holl and B. G. Orr, *Langmuir*, 2005, **21**, 10348–10354.
20 S. Parimi, T. J. Barnes and C. A. Prestidge, *Langmuir*, 2008, **24**, 13532–13539.
21 D. Stamou, C. Duschl, E. Delamarche and H. Vogel, *Angew. Chem., Int. Ed.*, 2003, **42**, 5580–5583.
22 W. Curatolo, B. Sears and L. J. Neuringer, *Biochim. Biophys. Acta*, 1985, **817**, 261–270.
23 P. Garidel, C. Johann, L. Mennicke and A. Blume, *Eur. Biophys. J.*, 1997, **26**, 447–459.
24 B. P. Navas, K. Lohner, G. Deutsch, S. Sevcsik, K. A. Riske, R. Dimova, P. Garidel and G. Pabst, *Biophys. Acta, Biomembr.*, 2005, **1716**, 40–48.
25 J. P. Reeves and R. M. Dowben, *J. Cell. Physiol.*, 1969, **73**, 49.
26 D. Needham and E. Evans, *Anal. Biochem.*, 1988, **27**, 8261–8269.
27 H. Lee and R. G. Larson, *J. Phys. Chem. B*, 2006, **110**, 18204–18211.
28 S. D. Shoemaker and T. K. Vanderlick, *Biophys. J.*, 2003, **84**, 998–1009.
29 M. V. Lizenko, T. I. Regerand, A. M. Bakhirev and E. I. Lizenko, *J. Evol. Biochem. Physiol.*, 2011, **47**, 428–437.
30 R. M. Epand and R. F. Epand, *Mol. BioSyst.*, 2009, **5**, 580–587.
31 A. Akesson, K. M. Bendtsen, M. A. Beherens, J. S. Pedersen, V. Alfredsson and M. C. Gomez, *Phys. Chem. Chem. Phys.*, 2010, **12**, 12267–12272.
32 K. Gardikis, S. Hatziantoniou, K. Viras, M. Wagner and C. Demetzos, *Int. J. Pharm.*, 2006, **318**, 118–123.
33 R. V. Diemel, M. M. E. Snel, A. J. Waring, F. J. Walther, L. M. G. van Golde, G. Putz, H. P. Haagsman and J. J. Batenburg, *J. Biol. Chem.*, 2002, **277**, 21179–21188.
34 H. Nakahara, S. Lee and O. Shibata, *Biophys. J.*, 2009, **96**, 1415–1429.
35 C. V. Kelly, M. G. Liroff, L. D. Triplett, P. R. Leroueil, D. G. Mullen, J. M. Wallace, S. Meshinchi, J. R. Baker, B. G. Orr and M. M. B. Holl, *ACS Nano*, 2009, **3**, 1886–1896.
36 L. Limozin and K. Sengupta, *ChemPhysChem*, 2009, **10**, 2752–2768.
37 F. Hook, B. Kasemo, T. Nylander, C. Fant, K. Sott and H. Elwing, *Anal. Chem.*, 2001, **73**, 5796–5804.
38 M. V. Voinova, M. Rodahl, M. Jonson and B. Kasemo, *Physica Scripta*, 1999, **59**, 391–396.
39 F. Hook, M. Rodahl, P. Brzezinski and B. Kasemo, *J. Colloid Interface Sci.*, 1998, **208**, 63–67.
40 F. Hook, M. Rodahl, P. Brzezinski and B. Kasemo, *Langmuir*, 1998, **14**, 729–734.
41 F. Hook, M. Rodahl, B. Kasemo and P. Brzezinski, *Proc. Natl. Acad. Sci. U. S. A.*, 1998, **95**, 12271–12276.
42 C. A. Keller and B. Kasemo, *Biophys. J.*, 1998, **75**, 1397–1402.
43 M. Edvardsson, S. Svedhem, G. Wang, R. Richter, M. Rodahl and B. Kasemo, *Anal. Chem.*, 2009, **81**, 349–361.

44 R. Richter, A. Mukhopadhyay and A. Brisson, *Biophys. J.*, 2003, **85**, 3035–3047.
45 C. Wang and K. C. Tam, *Langmuir*, 2002, **18**, 6484–6490.
46 C. V. Kelly, P. R. Leroueil, E. K. Nett, J. M. Wereszczynski, J. R. Baker, B. G. Orr, M. M. B. Holl and I. Andricioaei, *J. Phys. Chem. B*, 2008, **112**, 9337–9345.
47 C. V. Kelly, P. R. Leroueil, B. G. Orr, M. M. B. Holl and I. Andricioaei, *J. Phys. Chem. B*, 2008, **112**, 9346–9353.
48 S. Svenson and D. A. Tomalia, *Adv. Drug Delivery Rev.*, 2005, **57**, 2106–2129.
49 A. Mecke, I. Lee, J. R. Baker, M. M. B. Holl and B. G. Orr, *Eur. Phys. J. E: Soft Matter Biol. Phys.*, 2004, **14**, 7–16.
50 G. Stengel, L. Simonsson, R. A. Campbell and F. Hook, *J. Phys. Chem. B*, 2008, **112**, 8264–8274.
51 P. M. Bendix, M. S. Pedersen and D. Stamou, *Proc. Natl. Acad. Sci. U. S. A.*, 2009, **106**, 12341–12346.
52 Z. Y. Zhang and B. D. Smith, *Bioconjugate Chem.*, 2000, **11**, 805–814.
53 L. Albertazzi, M. Serresi, A. Albanese and F. Beltram, *Mol. Pharmaceutics*, 2010, **7**, 680–688.
54 M. P. Monopoli, D. Walczyk, A. Campbell, G. Elia, I. Lynch, F. B. Bombelli and K. A. Dawson, *J. Am. Chem. Soc.*, 2011, **133**, 2525–2534.
55 M. Lundqvist, J. Stigler, T. Cedervall, T. Berggard, M. B. Flanagan, I. Lynch, G. Elia and K. Dawson, *ACS Nano*, 2011, **5**, 7503–7509.
56 A. Salvati, C. Aberg, T. dos Santos, J. Varela, P. Pinto, I. Lynch and K. A. Dawson, *J. Nanomed. Nanotechnol.*, 2011, **7**, 818–826.
57 N. Malik, R. Wiwattanapatapee, R. Klopsch, K. Lorenz, H. Frey, J. W. Weener, E. W. Meijer, W. Paulus and R. Duncan, *J. Controlled Release*, 2000, **65**, 133–148.
58 B. Klajnert, S. Pikala and M. Bryszewska, *Proc. R. Soc. A*, 2010, **466**, 1527–1534.
59 D. Shcharbin, A. Drapeza, V. Loban, A. Lisichenok and M. Bryszewska, *Cell. Mol. Biol. Lett.*, 2006, **11**, 242–248.
60 S. P. Hong, A. U. Bielinska, A. Mecke, B. Keszler, J. L. Beals, X. Y. Shi, L. Balogh, B. G. Orr, J. R. Baker and M. M. B. Holl, *Bioconjugate Chem.*, 2004, **15**, 774–782.
61 Y. Ghetler, S. Yavin, R. Shalgi and A. Arav, *Hum. Reprod.*, 2005, **20**, 3385–3389.
62 S. W. Hui and D. F. Parsons, *Cancer Res.*, 1976, **36**, 1918–1922.

